PARALLEL ASSEMBLY OF COLLAGEN FIBRILS ON MICA SURFACE AND STEPS

A Senior Scholars Thesis

by

WEE WEN LEOW

Submitted to the Office of Undergraduate Research at
Texas A&M University
in partial fulfillment of the requirements for the designation as

UNDERGRADUATE RESEARCH SCHOLAR

April 2010

Major: Biomedical Engineering

PARALLEL ASSEMBLY OF COLLAGEN FIBRILS ON MICA SURFACE AND STEPS

A Senior Scholars Thesis

by

WEE WEN LEOW

Submitted to the Office of Undergraduate Research at
Texas A&M University
in partial fulfillment of the requirements for the designation as

UNDERGRADUATE RESEARCH SCHOLAR

Approved by:

Research Advisor: Wonmuk Hwang
Associate Dean for Undergraduate Research: Robert C. Webb

April 2010

Major: Biomedical Engineering

ABSTRACT

Parallel Assembly of Collagen Fibrils on Mica Surface and Steps. (April 2010)

Wee Wen Leow
Department of Biomedical Engineering
Texas A&M University

Research Advisor: Dr. Wonmuk Hwang
Department of Biomedical Engineering

Collagen is the most abundant protein in human body and the major component of the extracellular matrix. It self-assembles into fibrillar structures that exhibit characteristic 67-nm bands called the D-period. Despite decades of research, the molecular mechanism by which collagens assemble into ordered fibrillar structures is not well-understood. In this work, self-assembly of type-I collagen molecules in vitro was monitored using atomic force microscopy at different time points under various conditions. Control parameters include: monomer concentrations, pH, types of electrolytes, ionic strength, and incubation temperature. Presence of potassium and phosphate ions, and prolonged incubation were found to be essential for the formation of D-periods on the fibril. When assembled on a mica surface, the growth was fast and almost unlimited in the longitudinal direction but relatively slow in the direction transverse to the fibril axis. This resulted in fibrils aligning in parallel on mica surface. The spacing between collagen fibrils decreased over time. We also observed collagen assembly near regions containing steps on mica. At narrow steps (approximately 700 nm wide), collagen fibrils grew along the direction of the crack. However, for a shallow step (about 15 nm height), we observed collagens covering the crack, presumably because the thermal fluctuation of collagen was sufficient enough

to overcome the height of the step. Further studies are necessary to elucidate the possible assembly patterns and underlying mechanisms of collagen assembly at surface boundaries, which will be useful for developing defined matrices for biomaterial applications.

DEDICATION

To Hean Pin Leow, Hwee Tiang Tan

ACKNOWLEDGMENTS

I would like to thank my research advisor, Dr. Wonmuk Hwang, for his patience, guidance and support throughout the course of this research. I thank Sirish Kaushik Lakkaraju and Krishnakumar Mayuram Ravikumar for their input at various junctures of this project and the help on LaTex. Finally, I also thank my friends here at College Station for supporting me throughout this project.

TABLE OF CONTENTS

Page

LIST OF TABLES

LIST OF FIGURES

FIGURE Page

CHAPTER I

INTRODUCTION

Collagen is the most abundant structural protein found in mammals. There are more than 27 specialized collagens exist in mammalian tissue, which can form insoluble fibrous networks to provide structural support and form the extracellular matrix (ECM) in the body [1]. Collagen also provides scaffold which is functionalized by other ECM protein and plays an important role in cell interactions, attachment, tissue structuring, and is closely related to various human diseases [2, 3]. In addition, collagen has received considerable interest because of its applications in tissue engineering for two- and three-dimensional synthetic cell scaffolds [4, 5]. Collagen is also frequently used to coat non-biological surfaces to enhance bio-compatibility [6] and for functionalized surface patterning [7, 8]. In fact, collagen has been proven to be potentially useful in microelectronics application, where silicon nanowires can be created by utilizing the self-assembly properties of collagen molecules [9]. Collagen has been widely studied for over 6 decades, but the mechanism of its self assembly into ordered fibrils remains poorly understood. Some of the connective tissues from type I collagen in human body are well ordered, specific examples include corneal tissue [10] and tendon tissue [11]. It has been shown that scar tissue formation in the wound site is due to the poor quality of the restored collagen network [12], which can be related to the different assembly mechanism of the scar tissue versus normal tissue. It is hence important to understand the underlying molecular mechanisms of collagen assembly into fibrilar structure. Of many different techniques used in collagen study, atomic force microscopy (AFM) is widely used due to its exceptional sub-nano reso-

---

The journal model is *N*ature.

lution, high signal-to-noise ratio, and the superior advantage to investigate biological systems in aqueous environment, thereby preserving their physiological configurations and functions. AFM study on collagen fibrils was first reported by Chernoff and Chernoff [13] in 1992. Time-lapse imaging of collagen self-assembly on a surface has been studied by Cisneros et al. [14] The effects of pH and electrolytes on collagen assembly [15, 16], electrochemical and electric field guided collagen assembly [17, 18, 19] have also been studied. The effect of substrate, particularly mica, on the alignment of collagen fibrils was studied by Sun et al. [20] The effects of cationic and anionic substrates on the collagen adsorption were also studied on Gemini surfactant monolayers [21]. However, the alignment phenomena of these collagen fibrils on mica surface has not been adequately addressed in the previous studies. The significance of aligned collagen fibrils for cellular remodelling was studied by Friedrichs et al., where aligned collagen fibrils have anisotropic mechnical properties which may provide structural or signalling cues to cell polarization [22]. In this work, the self-assembly of type I collagen molecules on mica was observed using AFM. Collagen fibrils were observed to be highly aligned in a parallel manner on mica. Assembly patterns near regions containing cracks and steps on mica were also observed. By understanding the mechanism behind the collagen self assembly and alignment, collagen patterning can be achieved on a substrate to serve as a novel scaffold for biomaterial applications that may provide directional guide to cellular behaviors and differentiation.

A. Assembly of collagen fibrils

Type I collagen can self-assemble into fibrillar structure exhibiting characteristic 67-nm banding pattern. The self-assembly process is hierarchical, starting from collagen monomer, to microfibril, and subsequently to larger fibrils and networks (Fig. 1). The monomer, also known as tropocollagen, consists of three polypeptide chains (α-

chain) wound into a triple-helical structure with about 300 nm in length and 1.5 nm in diameter [23]. Five tropocollagen molecules form one microfibril which exhibits repeated banding pattern of gap and overlap regions, called the D-period. The D-period has been observed by Electron Microscopy (EM) [24], X-ray diffraction [25], and AFM [14, 26].

CHAPTER II

MATERIALS AND METHODS

The overview of the experimental procedures is shown in Fig. 2.

A. Collagen stock preparation

Two types of collagen stock were obtained due to the failure of the initial experiments in producing D-periods on collagen fibrils: Powder collagen prepared from lyophilized collagen and liquid collagen prepared from collagen solution.

1. Powder collagen

Collagen stock was prepared from lyophilized type I collagen derived from calf skin (MP Biomedicals 150026). 1 mg of lyophilized collagen was dissolved in 0.01 M acetic acid to 1 mg/ml. The mixture was sonicated at 4℃ for 1 hour (pH 3.5) and stored at 4℃ to be used for the experiments for up to 1 week.

2. Liquid collagen

Collagen stock was prepared from solubilized type I collagen derived from rat tail tendon (BD Biosciences 354236) (3.74 mg/ml) with >90% purity by SDS-PAGE. The aliquot was prepared by diluting the stock with 0.1% acetic acid to 1.65 mg/ml (pH 2.5) and stored at 4℃, and was used for experiments for up to 3 months.

B. Collagen assembly

Various collagen assembly protocols were tested in different experiments. The experiments are classified into 3 types: Collagen assembly without D-period, collagen assembly with D-period, and collagen assembly at mica cracks or steps. Control parameters include collagen concentration, presence of general electrolytes (potassium, sodium, magnesium, and chloride, excluding acids or bases used to adjust the

solution pH) and phophate ions, incubation temperature, substrate, and time. All AFM experiments were performed at room temperature. Experimental conditions are summarized in Table I.

1. Assembly without D-period

a. Low pH, no electrolyte

Powder collagen stock was diluted to 0.5 mg/ml with 0.01 M acetic acid for imaging. The pH of the imaging solution was 4.5. A 5-μl sample was deposited on freshly cleaved mica and incubated at room temperature for 1 minute. We used Kim wipes to remove the remaining solution at the mica edges and then set for air dry before imaging. This method of sample deposition on mica is termed A in Table I.

b. pH 6.5, no electrolyte

Powder collagen stock was diluted to 0.1 mg/ml by adding de-ionized (DI) water (18MΩ) and pH was adjusted by slowly adding aqeuous NaOH and HCl to give a final pH of 6.5. Method A was used to deposit sample on mica.

c. pH 7, with electrolyte

Collagen sample was prepared containing 0.1 mg/ml collagen from powder collagen stock, 100 mM KCl, 10 mM $MgCl_2$, and NaOH to adjust the pH to 7. 30-μl of the sample was deposited on the mica disk held at 45^o angle and Kim wipes were used to remove remaining solution at the mica edges and then set for air dry before imaging. This method of sample deposition is termed B in Table I.

d. pH 9, with electrolyte

Similar methods were employed as described in section B1c to yield collagen concentration of 0.02 mg/ml, KCl concentration of 200 mM at pH 9. In this case, sample was incubated in test tube at room temperature for 2.5 hours before imaging.

e. pH 7, with electrolyte, with phosphate ions

Aliquot from liquid collagen was used to prepare a sample containing 0.2 mg/ml collagen, 200 mM KCl, 20 mM of Na_2HPO_4, and 10 mM of KH_2PO_4. The pH of the sample was 7. Sample was incubated at 37℃ in test tube for 10 min. It was then diluted to 0.02 mg/ml with DI water, deposited on mica, and carefully rinsed twice with 90 μl of DI water to remove extra salt in the buffer and left to dry. This method of sample deposition is termed C in Table I. The incubation time on mica was 1 min.

2. Assembly with D-period

a. Collagen clumps

Sample prepared in section B1e was observed to form turbid solution after incubation at 37℃ for 30 min and clumps after a long period of time (>3 hours) set at room temperature. The clumps were carefully pipetted out from the solution and deposited on mica for 25 min. Method C was employed to deposit sample on mica.

b. Collagen monolayer

Collagen sample was prepared using liquid collagen stock to a final concentration of 0.05 mg/ml, containing 200 mM KCl, 30 mM Na_2HPO_4, and 10 mM KH_2PO_4. Sample was incubated at 37℃ for 30 min. 15-μl of sample was then deposited on mica and incubated at room temperature. Experiments were performed with 1 min, 10 min, and 108 min incubation time on mica. Method C was employed to deposit sample on mica.

3. Collagen assembly near boundaries

A freshly cleaved mica will contain some cracks or steps which can be imaged for collagen assembly behavior near the boundaries. Collagen sample was prepared as described in section B2b above. Sample was incubated on mica for prolonged period of time (>1 hour). Method C was employed to deposit sample on mica.

C. Atomic force microscopy (AFM)

Interleaved muscovite mica disks (Grade V1) were purchased from Ted Pella, Inc. Mica was fixed on a metal mounting disk and cleaved by sticky tape for each experiment. The AFM (AutoProbe CP-II, di-Veeco, CA) was operated in air at room temperature with 2 pizoelectric scanner: (i) Large Area Scanner with scan range 100 $\times$ 100 μm^2 and (ii) High Resolution Scanner with scan range 5 $\times$ 5 μm^2. Antimony doped silicon probe (Veeco Probes, FESP7) with nominal force constant of 2.8 N/m was employed in the entire experiments. Imaging was performed in Tapping Mode (NCM) at maximized NCM frequency near the the nomical resonance frequency of the cantilever (75 kHz). The signal to noise ratio was maintained at >10 and imaging was performed at NCM amplitude of about 70nm. The scanning speed was 1 Hz for small area scan (<2 μm) and decreased for larger area scan to ensure image quality. A 20$\times$ microscope was attached to the AFM machine to capture the area of the mica where the image was taken.

Image analysis and processing were performed in di-SPMLab. Only basic image processing including leveling and adjustment to the contrast histogram were done. Line analysis was performed to measure the heights and lengths of features in the data.

CHAPTER III

RESULTS

A. Collagen assembly without D-period

Fig. 3 compares collagen assembly without D-period under different conditions. Fig. 3(a) shows the AFM image of collagen at pH 4.5 under the condition described in section IIB1a. The globular structures show a height profile ranging from 2–5 nm, with the brighter spots possibly due to the stacking of collagen on top of each other. Fig. 3(b) shows the collagen under the condition described in section IIB1b, with the average height of each molecule <1 nm. The clump-like structure at the upper right of the image was possibly contamination in the sample or some undissolved collagen fibrils from the stock. Fig. 3(c) shows the first image obtained for self-assembly of collagen into fibrils under condition described in section IIB1c. The average height profile was 5 nm, with some fibrils stacking on each other. The horizontal lines present in the middle of the image was distortion due to the AFM tip disengaged during the scanning process and immediately adjusted by changing the drive percentage or the set point. Fig. 3(d) shows collagen fibril at pH 9 prepared as described in section IIB1d. The height of the fibrils ranges between 1–1.5 nm. Fig. 3(e) shows collagen fibril formed at neutral pH, with the presence of electrolytes and phosphate ions as described in section IIB1e. Dense collagen meshworks were observed but the collagen fibrils had no D-periodicity. The height of the fibrils was about 2.5 nm.

B. Collagen assembly with D-period

Sample prepared as described in section IIB2a was imaged with AFM, shown in Fig. 4(a). Image appeared blurry due to the tip interactions with the macroscopic features of the clump. Color contrast was performed in the rectangular box in the

image to highlight the banding on a fibril. The bottom of the image appeared shifted due to the signal distortion by the scanner. Banding patterns was observed with pitch-to-pitch distance approximately 54.6 nm as shown in Fig. 4(b).

Monolayer collagen assembly was achieved using methods described in section IIB2b. The collagen solution was incubated on mica surface immediately after incubation at 37℃ in test tube for 30 min, before the formation of clumps. Collagen assembled this way were observed to form parallel fibrils covering the mica surface, with very fast and almost unlimited longitudinal growth. Fig. 5 shows images taken at different incubation times on mica. The spacing between the fibrils were observed to decrease over time of incubation on mica. Fig. 5(a) shows highly aligned collagen fibril with 1 min incubation. No D-periods were observed at this point. D-banding was evident at 10 min incubation (Fig. 5(b)), with banding distance of 68.7 nm averaged over one fibril. Subsequently, the 108 min incubation point (Fig. 5(c)) shows very ordered collagen fibril monolayer on mica, with the spacing between fibrils significantly decreased compared to the 1 min incubation point. D-banding at 108 min incubation point shows the pitch-to-pitch distance of about 62.08 nm.

C. Collagen assembly near boundary

Fig. 6(a) was taken using 20× microscope, showing the AFM cantilever tip with laser spot and the area of the mica scanned. At a narrow crack, collagen fibrils were observed to assemble along the crack, as shown in Fig. 6(b). Multiple steps were observed in this image as the sharp lines presented on the scan, with the steps in the middle of the image defined as narrow crack. The cross-section of the narrow mica cracks (unleveled image) depicted the crack width as 713 nm and the step height as 25.97 nm (data not shown). Collagen fibrils in the narrow crack were observed to align parallel with each other and along the crack, whereas the collagen fibrils in

the upper plane were aligned in a different orientation, forming tapered ends at the boundary of the crack.

In another experiment with a shallow step as shown in Fig. 7(a), collagen fibrils assembled continuously across the step at the boundary. Collagen fibrils on the left and right planes were assembled and aligned in the same direction, with the fibrils on the left plane appearred to hang over the step. The bottom of Fig. 7(a) shows the cross section of the image, the height of the step is 14.75 nm and is defined as a shallow step in this study. No tapered ends were observed on the fibrils near the boundary, suggesting that the fibrils might be hanging over the shallow step, or possibly overcoming the barrier to merge with the fibrils on the other plane forming a continuous layer. As a comparison, another experiment was performed with greater mica step height and collagen fibrils were observed to be non-continuous, forming tapered ends at the step boundary, as shown in Fig. 7(b). The step height was measured to be 20.96 nm in this sample (data not shown).

AFM images scanned near the mica boundary were mostly dirty and unclear due to the dramatic topographic differences on the surface. Scanning was done under tapping mode in which the cantilever tip was oscillating right above the substrate and barely touching the surface. The tip's next movement was predicted based on the feedback from previous movements. Drastic changes in surface topograph will affect the quality of the scan as the tip cannot predict the next movement correctly and feed in wrong signal to the AFM controller program. In the case with drastic topographic changes, small features on the surface near the drastic change may possibly be omitted, thus creating a blurry area near the boundary.

CHAPTER IV

DISCUSSION

A. Collagen assembly without D-period

Trials and errors were performed to develop the correct protocol which yields collagen fibril with D-periods. The effects of pH and electrolytes on collagen assembly were previously studied [15]. Fig. 3(a) shows the collagen molecules adsorbed to mica as globular protrusions at pH 4.5 [15]. We think that due to the uneven charge distribution on collagen molecules, they were collapsed to hide the hydrophobic sidechains due to positive charge repulsion at low pH condition, forming globular structures. Once neutralized, individual tropocollagens can be seen, where no assembly occured due to the absence of essential electrolytes, i.e. potassium ions (Fig. 3(b)). The measured contour length of the tropoccollagen here is about 300 nm, comparable to the theoretical value, while the height was measured to be <1nm, which is less than the theoretical diameter for a collagen triple helix (1.5 nm) [23]. This discrepancy may be due to three reasons: (i) imaging was performed in dry and thus the drying force could have caused the molecules to collapse on the mica surface, (ii) force applied from the AFM tip during Tapping Mode imaging, (iii) the binding force between the molecule and the mica substrate. Similar AFM images on collagen monomer were shown in Bozec and Horton's work [27].

Upon addition of potassium ions, self-assembly of collagen begins spontaneously as shown in Fig. 3(c). The presence of ionic species including KCl and $MgCl_2$ has an electrostatic screening effect to the collagen monomer, shortening the Debey length thus allowing self-assembly of collagen. The effects of potassium ions on collagen assembly has been greatly studied previously [28, 15]. NaCl could have the same screening effect as KCl but the presence of potassium is needed for the formation of D-

period on mica [29]. Potassium ions play an important role in molecules assembly on mica due to the presence of K^+-binding pocket on mica surface [30]. Muscovite mica is composed of negatively charged aluminosilicate layers held together by the interlayer potassium ions. A cleaved mica surface can thus be expected to have potassium ions distributed equally over the two cleaved layers [31]. Potassium ions present in the collagen buffer will thus modulate the assembly of collagen fibrils by serving as a competitive inhibitor to collagen molecules to bind to the K^+-binding pocket on the mica surface. Compared to low pH case (pH 4.5), the electrostatic repulsion of collagen molecules was reduced to allow self-assembly at neutral pH (6.5–7). Effect of high pH (pH 9) was shown in Fig 3(c), yielding thinner fibrils. Phosphate ions which is thought to be essential to the collagen D-period formation was added in Fig. 3(e) at neutral pH together with potassium ions. However, D-periodicity did not appear for even up to 120 min (data not shown) sample incubation at 37℃, possibly due to the lack of a substrate for proper monolayer assembly of collagen fibril and insufficient time for collagen clumps with D-period to form.

B. Collagen assembly with D-period

The formation of D-bandings was first detected in collagen clumps formed visible to bare eye after prolonged incubation at 37℃ (30min) in test tube and room temperature for hours. Although Fig. 4(a) shows an average banding pattern of 54.6 nm which is less than the regular 67 nm D-periods observed in native type I collagen, shorter D-periods has been reported in other works [16]. Shorter D-periods could be due to the dehydration of the sample during the drying process. It could also be a transient structure that forms during the fibrogenesis process [16], in which the fibrils relax to a lower energy state. However, the actual D-period could be longer and more measurements are necessarily for a more accurate estimation of D-period.

Comparing different methods and protocols of collagen assembly, we concluded that the critical step in obtaining monolayer collagen assembly with D-period is to incubate the sample on a mica surface for a given amount of time depending on the monomer concentration. At a collagen concentration of 0.05 mg/ml with 30 min sample incubation in test tube at 37℃, D-periods were not formed until at least 10 min incubation on mica (Fig. 5(b)). At 1 min mica incubation, traces of D-periods were inevident (Fig. 5(a)). Surface assembly is then shown to be essential for obtaining collagen monolayer with D-periods because the sample incubated at 37℃ for 120 min in the test tube alone does not give rise to D-period formation, but only shows thin fibrils in meshworks similar to Fig. 3(e)(data not shown).

In Fig. 5(a), the 2 μm scan shows small and thin fibrils in the background. Comparing Fig. 5(a),(b), and (c), the background small fibrils decreased and the big collagen fibrils were more solid and packed over time. All three images were taken at the same collagen concentration. Also, we observed the spacing between the fibrils to decrease over time, showing that lateral growth was possible but much slower than the longitudinal growth since the fibrils appear to be highly aligned and long at even at 1 min incubation time on mica. To further understand how fast the longitudinal assembly can go, we have performed another experiment with 5 times dilution (0.01 mg/ml) of collagen (maintaining ionic strength and pH) and eliminated the 30 min incubation step at 37℃. The 1 min incubation of such sample on mica was shown in Fig. 8. We observed that collagen self-assembled into very long fibrils and well-aligned on mica even at 1 min incubation on mica, without prior incubation in test tube at 37℃.

Another interesting phenomenon we observed was the high order and alignment of collagen fibrils on mica. As a control, we incubated the same collagen sample on other substrates such as silicon wafer (Fig. 9) and phlogopite mica (data not shown).

AFM topographies show random meshworks of collagen fibrils as opposed to the highly aligned fibrils on mica. We are currently studying the underlying reasons for the alignment. We propose two possible factors that can contribute to the alignment phenomena: (i) Mica lattice may serve as a template for collagen alignment, (ii) long-ranged interaction between collagen molecules might be the cause for the alignment. The first theory was proposed by Sun et al., who claimed that the distorted hexagonal symmetry of mica lattice could guide collagen alignment [20]. Kuwahara's work on mica surface structure reveals that once cleaved, dioctahedral muscovite mica experiences surface relaxation which is caused by a large tetrahedral rotation [32]. According to Kuwahara, this rotation then results in grooves from tetrahedral tilt, made by subsiding the basal oxygen connecting adjacent SiO_4 tetrahedra across the elongated edge in each distorted hexagonal ring [32]. In contrast, for trioctahedral mica (phlogopite), large tetahedral rotation does not occur because of a smaller lateral misfit and smaller interlayer cation [33]. Balzer et al. in the assembly study of organic oligomer proposed that it was the grooves present on muscovite mica surface which leads to the major direction for alignment of aggregates on muscovite mica [34].

However, the asymmetry of mica lattice may not the sole reason for collagen fibrils alignment on mica for two reasons: (i) The small and thin fibrils in the background of Fig. 8 were not aligned in the same orientation with each other, but only the bigger ones were, (ii) surface assembly must have occured while the sample is incubated on the mica surface as the collagen molecules diffused, packed, and aligned (lateral growth of the fibrils observed and the background small fibrils decreased), indicating that the molecules are not immobilized once adsorbed on mica surface. It is also unlikely that the alignment is due to drying or rinsing direction for the same reasons mentioned above. More careful experiments and analysis have to be carried out to better understand the assembly of parallelly aligned collagen layer.

Freshly-cleaved mica substrate contains K^+-binding pocket which is negatively charged. Collagen molecules at neutral pH are positively charged. Hence, once deposited on mica, collagen molecules will compete with the K^+ ions present in the buffer to adsorb to the mica surface. The correct binding rate has to be achieved for collagen to assemble into D-periodic structure. As a future work, we think that similar collagen assembly can be achieved on silicon substrate if one can tailor the correct buffer condition and make the silicon substrate negatively charged by applying slight electric potential.

C. Collagen assembly near boundary

The investigation on collagen assembly near mica boundary is limited with the resolution of AFM and also the difficulty in controlling the crack/ step width and height on mica. The mica disk was cleaved by peeling off the sticky tape on its surface to obtain a clean mica surface for every experiment. Thus, the cracks and steps on mica are random. Based on Fig. 6, different alignment of collagen fibrils can be achieved by having a step-like surface. Zhu et al. had fabricated nanogroves on polystyrene using polarized laser and showed that collagen fibrils aligned along the grooves [8]. Ability to generate aligned collagen matrix is desirable for understanding the effect of anisotropy of extracellular matrix (ECM) on cell behaviors.

Comparing Fig. 7 (a) and (b), thermal motion may cause the fibrils to overcome the step at the boundary when the step height is small, e.g. less than 15 nm. Tapered ends were not observed in Fig. 7(a) but in Fig. 7(b), which has a step height of about 21 nm. Fig. 6(b) shows tapered ends on the upper plane as well and the step height was about 26 nm.

CHAPTER V

SUMMARY AND CONCLUSION

This work higlighted various assembly conditions of type I collagen molecules on mica surface. We conclude that the citical conditions for monolayer collagen assembly on mica with D-periods are: (i) potassium ions, (ii) phosphate ions, and (iii) prolonged incubation on mica substrate. We propose that the assembly of collagen monolayer consists of three critical steps. The initial surface adsorption of the collagen molecules to the mica substrate, assisted by the presence of potassium ions which act as a competitive inhibitor to the K^+-binding pocket on the cleaved mica surface. The process is followed by the growth of the fibrils by addition of molecules to the existing ones, which we believe to be assisted by the presence of phosphate ions that mimics the physiological environment. The final step is the maturation or the rearrangement process, in which the collagen molecules rearrange themselves into energetically favorable confirmations to form a native-like microfibril, then hierarchically into fibrils which exhibit D-periodicity. When incubated on mica substrate, collagen molecules assemble into highly aligned fibrils with fast longitudinal growth and relatively slow lateral growth. It appears that the alignment of the fibrils was neither due to the hydrodynamic flow nor drying. Two factors affecting collagen alignment on mica include the effect of mica lattice and the long-range interactions between collagen molecules. More studies are needed to find out whether and how these factors operate. The structure and alignment of collagen fibrils play an important role in our body since some diseases such as canine myxomatous mitral valve disease are directly related to the misalignment of collagen [35]. Apart from that, information from collagen assembly near mica boundary can be useful in constructing *ex vivo* scaffold for biomaterials application. A more careful method has to be developed in creating defined steps on

mica to further study collagen assembly near boundary. As a future work, we will focus on understanding the mechanism for the long range alignment of collagen fibrils on mica.

REFERENCES

[1] Boot-Handford, R. P., Tuckwell, D. S., Plumb, D. A., Rock, C. F., and Poulsom, R. A Novel and Highly Conserved Collagen (pro1(XXVII)) with a Unique Expression Pattern and Unusual Molecular Characteristics Establishes a New Clade within the Vertebrate Fibrillar Collagen Family. *Journal of Biological Chemistry* **278**(33), 31067–31077 (2003).

[2] Akiyama, S. K., Nagata, K., and Yamada, K. M. Cell surface receptors for extracellular matrix components. *Biochimica et Biophysica Acta (BBA) - Reviews on Biomembranes* **1031**(1), 91–110 (1990).

[3] Kadler, K. Learning how mutations in type I collagen genes cause connective tissue disease. *International Journal of Experimental Pathology* **74**(4), 319–323 (1993).

[4] Guidry, C. and Grinnell, F. Studies on the mechanism of hydrated collagen gel reorganization by human skin fibroblast. *Journal of Cell Science* **79**(1), 67–81 (1985).

[5] Thomas, A., Campbell, G., and Campbell, J. Advances in vascular tissue engineering. *Cardiovascular Pathology* **12**(5), 271–276 (2003).

[6] Lee, C., Singla, A., and Lee, Y. Biomedical applications of collagen. *International Journal of Pharmaceutics* **221**(1-2), 1–22 (2001).

[7] Monroe, M., Li, Y., Ajinkya, S., Gower, L., and Douglas, E. Directed collagen patterning on gold-coated silicon substrates via micro-contact printing. *Materials Science and Engineering: C* **29**, 2365–2369 (2009).

[8] Zhu, B., Lu, Q., Yin, J., Hu, J., and Wang, Z. Alignment of osteoblast-like cells and cell-produced collagen matrix induced by nanogrooves. *Tissue Engineering* **11**(5-6), 825–834 (2005).

[9] Salhi, B., Vaurette, F., Grandidier, B., Stiévenard, D., Melnyk, O., Coffinier, Y., and Boukherroub, R. The collagen assisted self-assembly of silicon nanowires. *Nanotechnology* **20**, 235601–235607 (2009).

[10] Holmes, D., Gilpin, C., Baldock, C., Ziese, U., Koster, A., and Kadler, K. Corneal collagen fibril structure in three dimensions: Structural insights into fibril assembly, mechanical properties, and tissue organization. *Proceedings of the National Academy of Sciences* **98**(13), 7307–7312 (2001).

[11] Traub, W., Arad, T., and Weiner, S. Three-dimensional ordered distribution of crystals in turkey tendon collagen fibers. *Proceedings of the National Academy of Sciences of the United States of America* **86**(24), 9822–9826 (1989).

[12] van Zuijlen, P., Ruurda, J., van Veen, H., van Marle, J., van Trier, A., Groenevelt, F., Kreis, R., and Middelkoop, E. Collagen morphology in human skin and scar tissue: no adaptations in response to mechanical loading at joints. *Burns* **29**(5), 423–431 (2003).

[13] Chernoff, E. and Chernoff, D. Atomic force microscope images of collagen fibers. *Journal of Vacuum Science & Technology A: Vacuum, Surfaces, and Films* **10**, 596–599 (1992).

[14] Cisneros, D., Hung, C., Franz, C., and Muller, D. Observing growth steps of collagen self-assembly by time-lapse high-resolution atomic force microscopy. *Journal of structural biology* **154**(3), 232–245 (2006).

[15] Jiang, F., Horber, H., Howard, J., and Muller, D. Assembly of collagen into microribbons: effects of pH and electrolytes. *Journal of Structural Biology* **148**(3), 268–278 (2004).

[16] Li, Y., Asadi, A., Monroe, M., and Douglas, E. pH effects on collagen fibrillogenesis in vitro: Electrostatic interactions and phosphate binding. *Materials Science and Engineering: C* **29**(5), 1643–1649 (2009).

[17] Huelin, S., Baker, H., Poduska, K., Merschrod, S., and Erika, F. Aggregation and adsorption of type I collagen near an electrified interface. *Macromolecules* **40**(23), 8440–8444 (2007).

[18] Baker, H. and Poduska, K. Electrochemically controlled growth and positioning of suspended collagen membranes. *Langmuir* **24**(7), 2970–2972 (2008).

[19] Cheng, X., Gurkan, U., Dehen, C., Tate, M., Hillhouse, H., Simpson, G., and Akkus, O. An electrochemical fabrication process for the assembly of anisotropically oriented collagen bundles. *Biomaterials* **29**(22), 3278–3288 (2008).

[20] Sun, M. and Stetco, A. Surface-templated formation of protein microfibril arrays. *Langmuir* **24**(10), 5418–5421 (2008).

[21] Xu, S., Liu, A., Chen, Q., Lv, M., Yonese, M., and Liu, H. Self-assembly nano-structure of type I collagen adsorbed on Gemini surfactant LB monolayers. *Colloids and Surfaces B: Biointerfaces* **70**(1), 124–131 (2009).

[22] Friedrichs, J., Taubenberger, A., Franz, C. M., and Muller, D. J. Cellular remodelling of individual collagen fibrils visualized by time-lapse afm. *Journal of Molecular Biology* **372**(3), 594–607 (2007).

[23] Kadler, K., Holmes, D., Trotter, J., and Chapman, J. Collagen fibril formation. *Biochemical Journal* **316**(Pt 1), 1–11 (1996).

[24] Williams, B., Gelman, R., Poppke, D., and Piez, K. Collagen fibril formation. Optimal in vitro conditions and preliminary kinetic results. *Journal of Biological Chemistry* **253**(18), 6578–6585 (1978).

[25] Orgel, J. P., Miller, A., Irving, T. C., Fischetti, R. F., Hammersley, A. P., and Wess, T. J. The in situ supermolecular structure of type i collagen. *Structure* **9**(11), 1061–1069 (2001).

[26] Gale, M., Pollanen, M., Markiewicz, P., and Goh, M. Sequential assembly of collagen revealed by atomic force microscopy. *Biophysical Journal* **68**(5), 2124–2128 (1995).

[27] Bozec, L. and Horton, M. Topography and mechanical properties of single molecules of type I collagen using atomic force microscopy. *Biophysical Journal* **88**(6), 4223–4231 (2005).

[28] Loo, R. and Goh, M. Potassium ion mediated collagen microfibril assembly on mica. *Langmuir* **24**(23), 13276–13278 (2008).

[29] Cisneros, D., Friedrichs, J., Taubenberger, A., Franz, C., and Muller, D. Creating ultrathin nanoscopic collagen matrices for biological and biotechnological applications. *Small* **3**(6), 956–963 (2007).

[30] Karsai, A., Murvai, U., Soos, K., Penke, B., and Kellermayer, M. Oriented epitaxial growth of amyloid fibrils of the N27C mutant β25–35 peptide. *European Biophysics Journal* **37**(7), 1133–1137 (2008).

[31] Ostendorf, F., Schmitz, C., Hirth, S., Kuhnle, A., Kolodziej, J., and Reichling, M. How flat is an air-cleaved mica surface? *Nanotechnology* **19**, 305705–305711 (2008).

[32] Kuwahara, Y. Muscovite surface structure imaged by fluid contact mode AFM. *Physics and Chemistry of Minerals* **26**(3), 198–205 (1999).

[33] Kuwahara, Y. Comparison of the surface structure of the tetrahedral sheets of muscovite and phlogopite by AFM. *Physics and Chemistry of Minerals* **28**(1), 1–8 (2001).

[34] Balzer, F., Kankate, L., Niehus, H., and Rubahn, H. Epitaxy vs. dipole assisted growth for organic oligomer nanoaggregates. In *Proceedings of SPIE*, volume 5925, 59250A, (2005).

[35] Hadian, M., Corcoran, B., Han, R., Grossmann, J., and Bradshaw, J. Collagen organization in canine myxomatous mitral valve disease: an x-ray diffraction study. *Biophysical Journal* **93**(7), 2472–2476 (2007).

APPENDIX

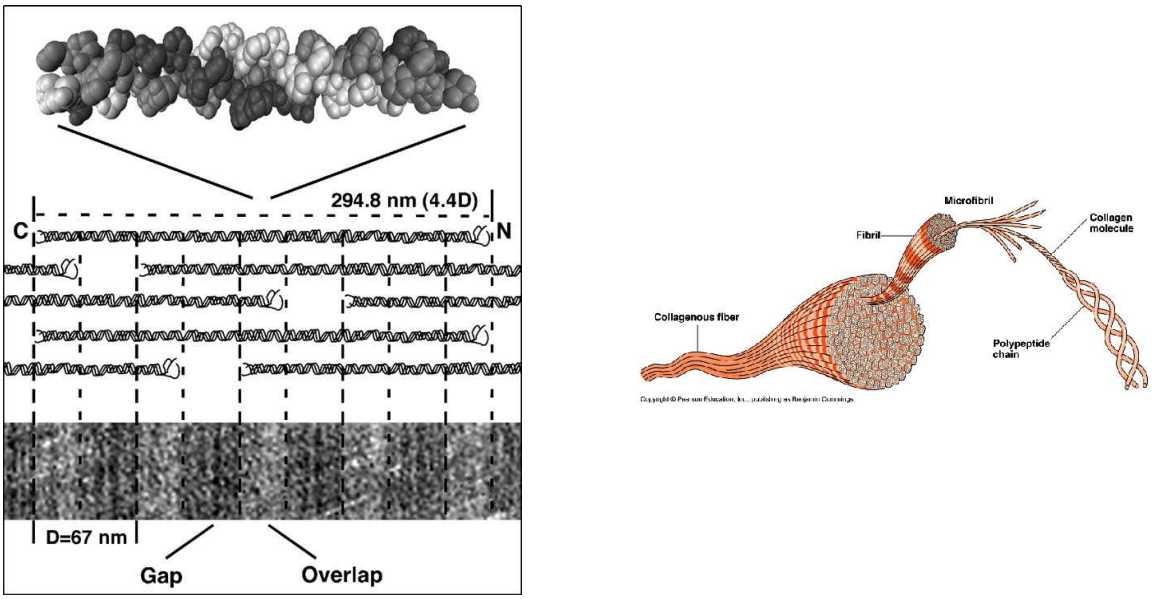

(a) (b)

Fig. 1. Model of the hierarchical assembly of type I collagen. (a) From top: Tropocollagen about 300 nm in length. Five of them stagger laterally to form one microfibril with repeating gap and overlap regions. One gap and overlap is 67 nm in length. Image adopted from Cisneros et al. (b) A schema showing hierarchical nature of collagen assemblies, image from Campbell et al.

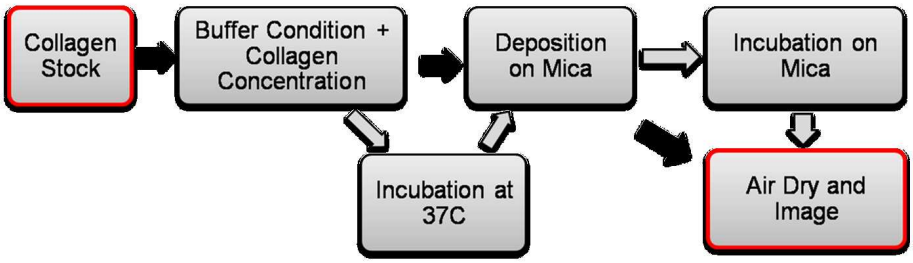

Fig. 2. Overview of the exprimental procedure. Collagen stock was obtained and adjusted to a desired concentration and buffer conditions, deposition on mica, and air dried to be imaged with AFM. Incubation of sample at 37℃ in test tube or at room temperature on mica was optional and was part of the parameters in the study.

Table I. Summary of different experimental setups. (RT stands for room temperature in this context)

Section	Subsections	Collagen Stock	Collagen Conc. (mg/ml)	pH	Electrolytes		Phosphate ions		37°C Incub. (min)	RT Incub. (min)	Mica Deposit	Mica Incub. (min)
					KCl (mM)	$MgCl_2$ (mM)	Na_2HPO_4 (mM)	KH_2PO_4 (mM)				
B1a	Low pH, no electrolyte	Powder	0.5	4.5	-	-	-	-	-	-	A	-
B1b	pH6.5, no electrolyte	Powder	0.1	6.5	-	-	-	-	-	-	A	-
B1c	pH7, w/ electrolyte	Powder	0.1	7	100	10	-	-	-	-	B	-
B1d	pH9, w/ electrolyte	Powder	0.02	9	200	-	-	-	-	150	B	-
B1e	pH7, w/ electrolyte, w/ phosphate	Liquid	0.02	7	200	-	20	10	10	-	C	1
B2a	Clumps	Liquid	0.2	7	200	-	20	10	30	>3 hr	C	25
B2b	Monolayer	Liquid	0.05	7	200	-	30	10	30	-	C	1
		Liquid	0.05	7	200	-	30	10	30	-	C	10
		Liquid	0.05	7	200	-	30	10	30	-	C	108
B3a	-	Liquid	0.05	7	200	-	30	10	30	-	C	>1 hr

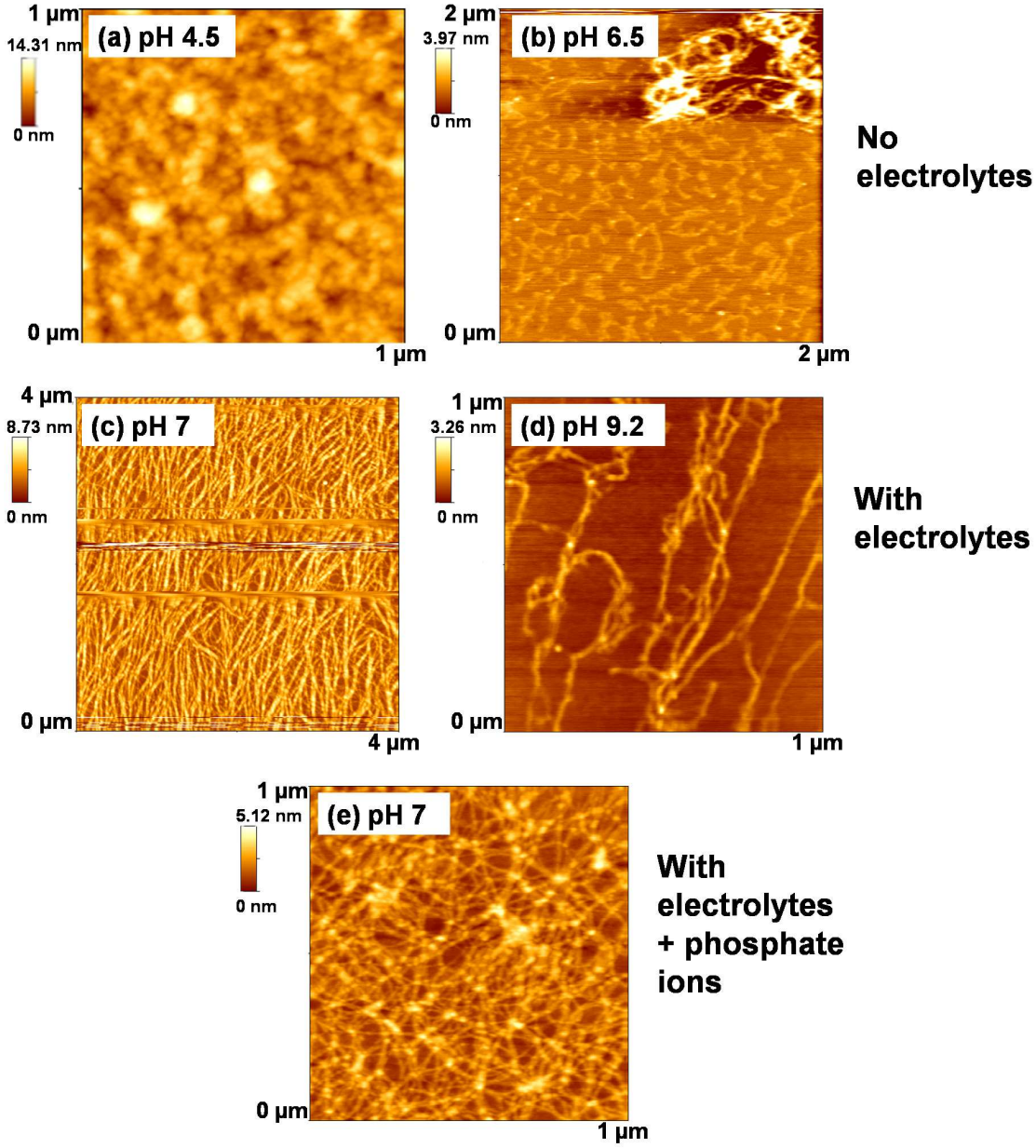

Fig. 3. AFM images of collagen assembly without D-period at different conditions (see Table I). (a) At low pH and no electrolyte, 0.5 mg/ml collagen. (b) Neutral pH and no electrolyte, 0.1 mg/ml collagen. (c) First collagen fibrils formation at neutral pH and with electrolyte, 0.1 mg/ml collagen. (d) At pH 9 and with electrolyte, 0.02 mg/ml collagen. (e) At neutral pH, with electrolyte and phosphate buffer, 0.02 mg/ml collagen, incubated for 10 min at 37℃.

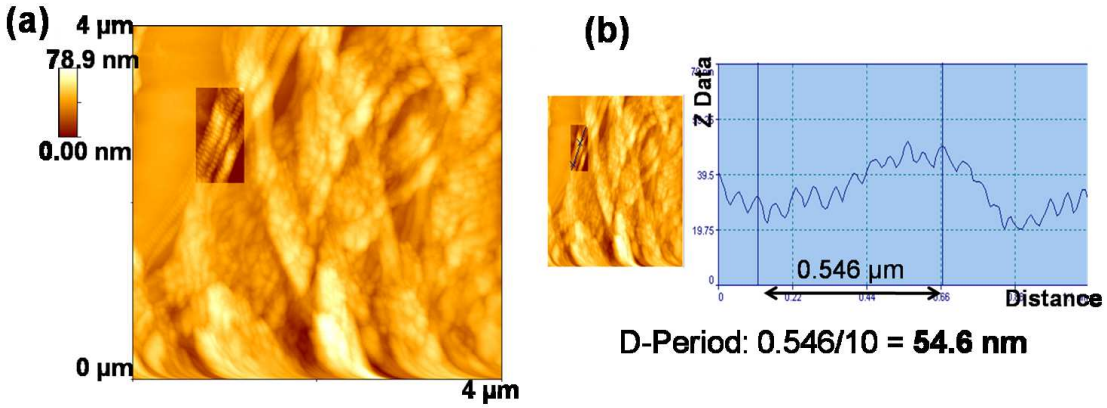

Fig. 4. AFM images of collagen assembly with D-period. (a) Collagen clumps observed with D-periods. (b) Line analysis of the collagen fibril in the clump showing the evidence of repeating periodicity, approximately 54.6 nm.

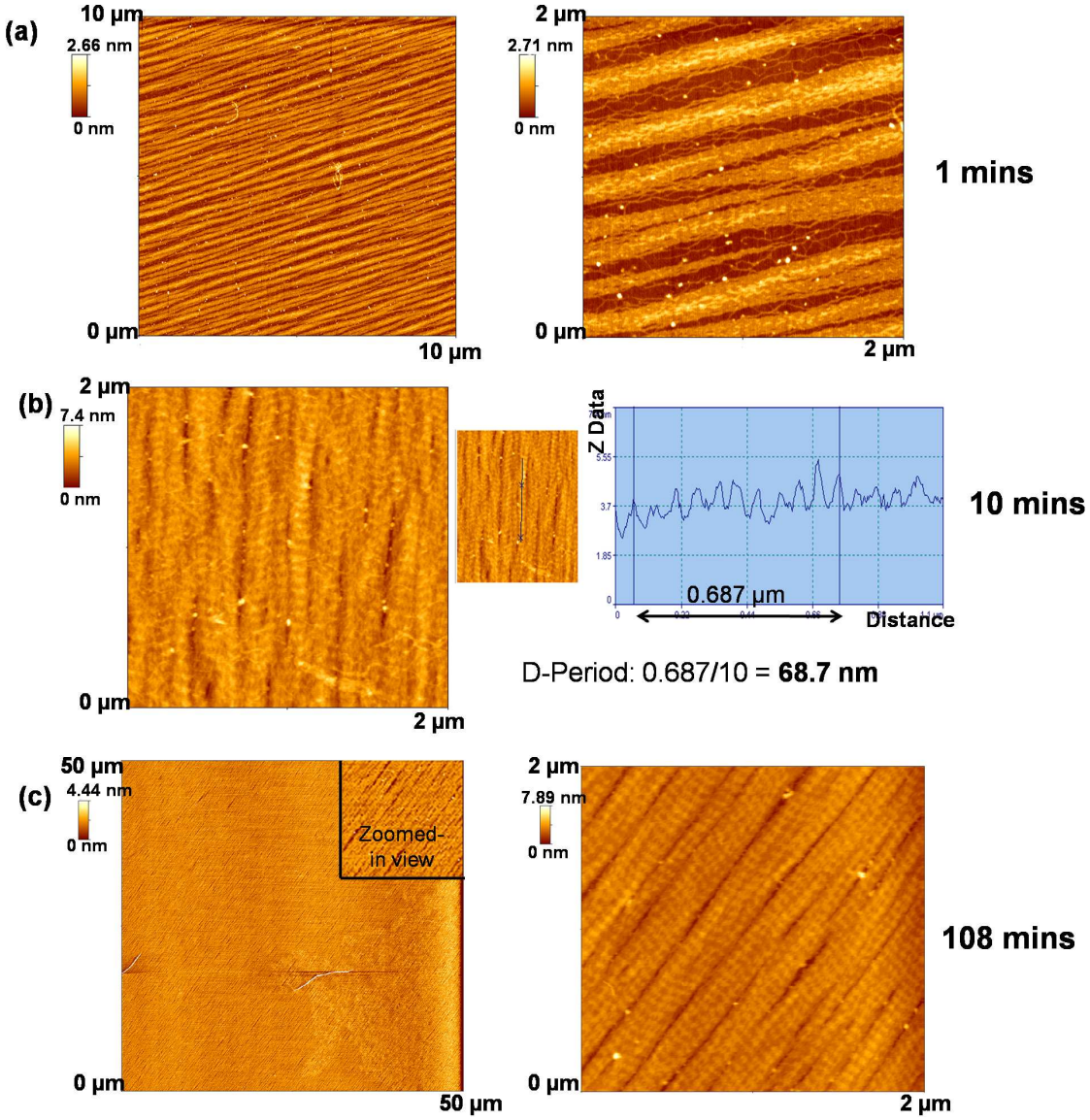

Fig. 5. Layers of collagen fibrils formed after 30 min incubation in test tube at 37°C and (a) 1 min incubation on mica at RT, right: zoom-in view, approximate height of small fibril in the background less than 1 nm, big fibril= 1–2 nm; (b) 10 min on mica. Right: line analysis of a fibril, showing banding about 68.7 nm, fibril height= 2–4 nm; (c) 108 min on mica. Left: 50×50 μm^2 (top right corner shows a digital zoom in). Right: zoom-in scan, fibril height= 2–3 nm, banding about 62.08 nm.

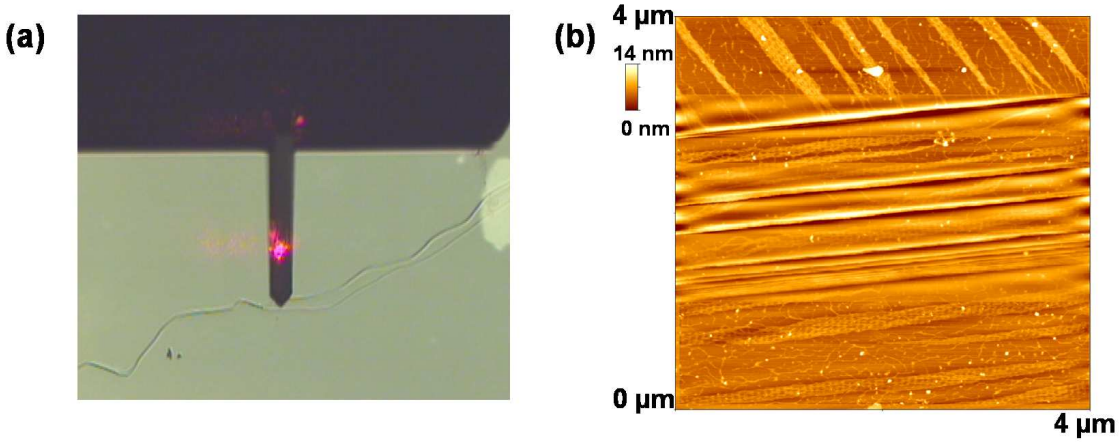

Fig. 6. Collagen assembly near narrow mica crack/ step. (a) Microscope image of the mica crack area scanned with AFM, 20× magnification. (b) AFM topography near a narrow crack (mica step boundary). Different collagen alignment was observed at the narrow step and the upper and lower plane, collagen fibrils were aligned along the narrow step. Crack width was measured as 713 nm and step height was 25.97 nm.

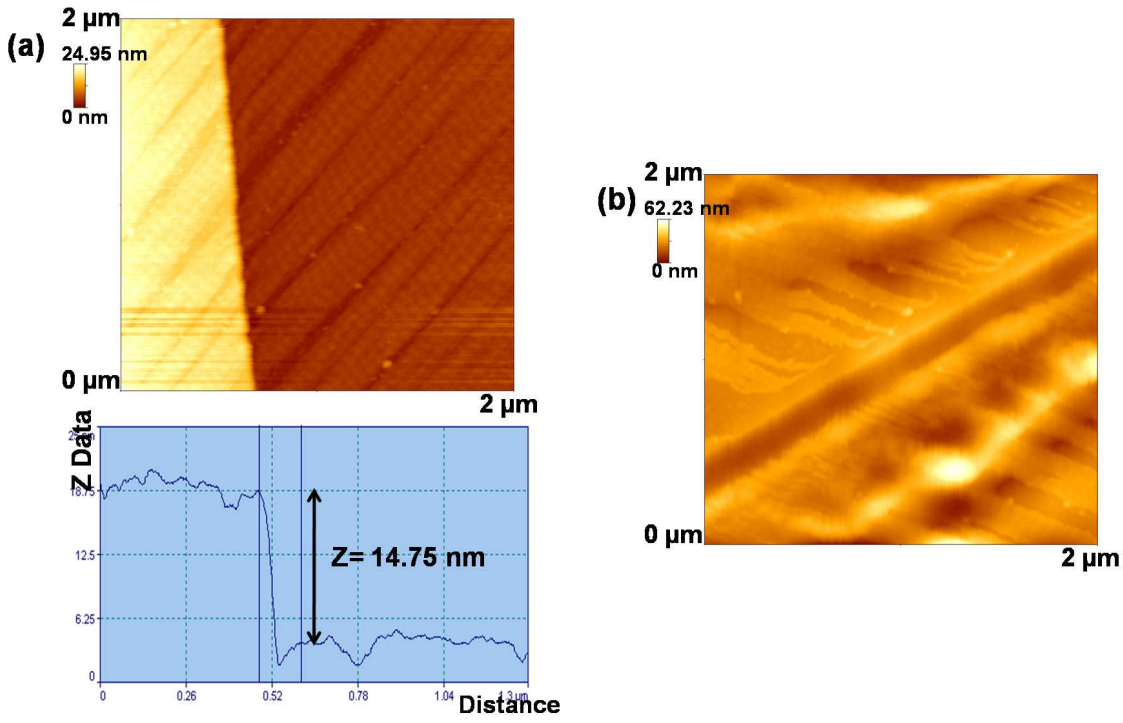

Fig. 7. Collagen assembly near shallow mica crack/ step. (a) Top: AFM topography. Note that collagen alignment was the same across the boundary; bottom: cross-sectional view of the step. (b) Collagen assembly at deeper mica step boundary. Collagen alignment was the same observed at the upper and lower plane of the boundary but the ends of the fibrils near the boundary were tapered. The mica step height was about 20.96 nm.

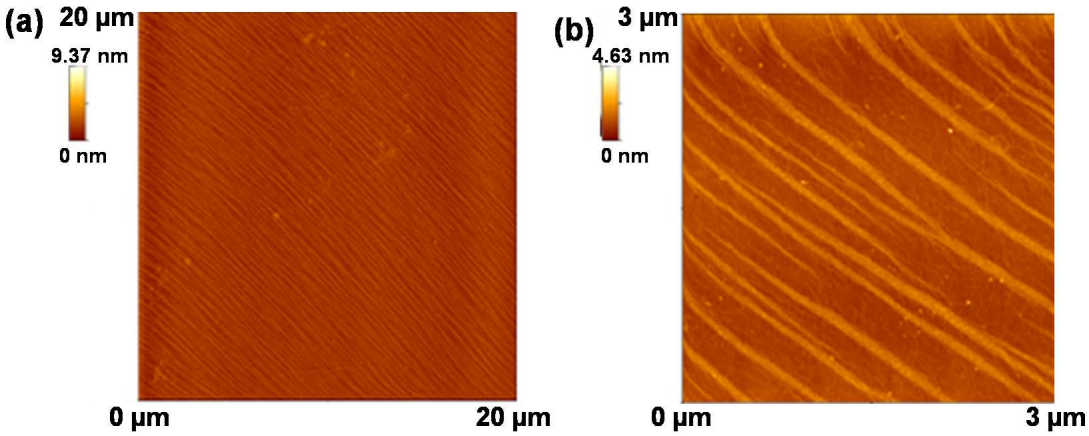

Fig. 8. Monolayer collagen assembly with no 37℃ incubation in test tube. Collagen concentration was 0.01 mg/ml and incubated 1 min at room temperature on mica. (a) 20 X 20 μm^2 scan and (b)3 X 3 μm^2 scan.

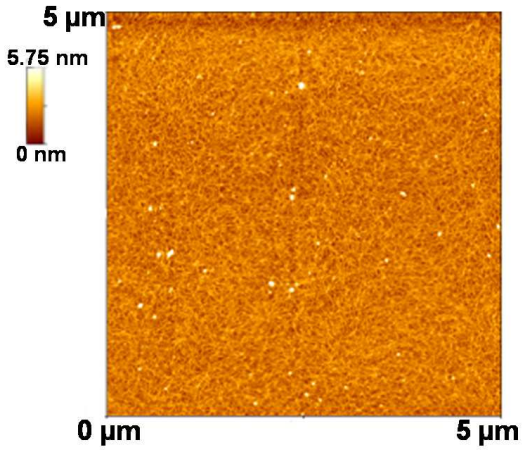

Fig. 9. 0.05 mg/ml collagen assembled on piranha treated silicon wafer. Sample was incubated at room temperature for 30 min in test tube followed by 20 min on silicon wafer prior to imaging.

CONTACT INFORMATION

Name:	Wee Wen Leow
Address:	337 Zachary Engr. Ctr, 3120 TAMU, College Station, TX 77843
Email Address:	weewenleow@neo.tamu.edu
Education:	B.S. Biomedical Engineering, Texas A&M University, 2009

The typist for this thesis was Wee Wen Leow.